Title

Detection of cerebral reorganization associated with degenerative cervical myelopathy using diffusion spectral imaging (DSI)

Authors

Wang, Chencai
Holly, Langston T
Oughourlian, Talia
et al.

Publication Date

2021-04-01

DOI

10.1016/j.jocn.2021.01.011

Peer reviewed

HHS Public Access

Author manuscript

J Clin Neurosci. Author manuscript; available in PMC 2022 April 01.

Published in final edited form as:

J Clin Neurosci. 2021 April ; 86: 164–173. doi:10.1016/j.jocn.2021.01.011.

Detection of cerebral reorganization associated with degenerative cervical myelopathy using diffusion spectral imaging (DSI)

Chencai Wang, Ph.D.[a], **Langston T. Holly, M.D.**[b], **Talia Oughourlian, B.S.**[a,c], **Jingwen Yao, M.S.**[a], **Catalina Raymond, M.S.**[a], **Noriko Salamon, M.D.**[a], **Benjamin M. Ellingson, Ph.D.**[a,c,d]

[a]Dept. of Radiological Sciences, David Geffen School of Medicine, University of California Los Angeles, Los Angeles, CA

[b]Dept. of Neurosurgery, David Geffen School of Medicine, University of California Los Angeles, Los Angeles, CA

[c]Neuroscience Interdisciplinary Graduate Program, David Geffen School of Medicine, University of California Los Angeles, Los Angeles, CA

[d]Dept. of Psychiatry and Biobehavioral Sciences, David Geffen School of Medicine, University of California Los Angeles, Los Angeles, CA

Abstract

Degenerative Cervical Myelopathy (DCM) is a spinal cord disorder that causes significant physical disabilities in older patients. While most DCM research focuses on the spinal cord, widespread reorganization of the brain may occur to compensate for functional impairment. This observational study used diffusion spectrum imaging (DSI) to examine reorganization of cerebral white matter associated with neurological impairment as measured by the modified Japanese Orthopedic Association (mJOA), and severity of neck disability as measured by the Neck Disability Index (NDI) score. A total of 47 patients were included in the cervical spondylosis (CS) cohort: 38 patients with DCM (mean mJOA=14.6, and mean NDI=12.0), and 9 neurologically asymptomatic patients with spinal cord compression (mJOA=18, and mean NDI=7.0). 28 healthy volunteers (HCs) served as the control group. Lower generalized fractional anisotropy (GFA) was observed throughout much of the brain in patients compared to HCs ($p<0.05$). Fiber pathways associated with somatosensory functions, such as the corpus callosum and corona radiata, showed increased quantitative anisotropy (QA) in patients compared to HCs. Correlation analyses further suggested that structural connectivity was enhanced to compensate for neurological dysfunction within sensorimotor regions, where fibers such as the posterior corona radiata had NQA values that were negatively associated with mJOA ($p=0.0020$, $R^2=0.2935$) and positively associated with

Address Correspondence To: Benjamin M. Ellingson, Ph.D., Professor of Radiology, Biomedical Physics, Bioengineering, and Psychiatry, Departments of Radiological Sciences and Psychiatry, David Geffen School of Medicine, University of California – Los Angeles, 924 Westwood Blvd, Suite 615, Los Angeles, CA 90024.

Conflicts of Interest: None

NDI score (p=0.0164, R^2=0.1889). Altogether, these results suggest that DCM and neurologically asymptomatic spinal cord compression patients tend to have long-term reorganization within the brain, particularly in those regions responsible for the perception and integration of sensory information, motor regulation, and pain modulation.

Keywords

Diffusion spectral imaging; Degenerative cervical myelopathy; Cervical spondylosis

1. Introduction

Cervical spondylosis (CS) is an age-related degenerative spine condition in which long-term deterioration and dehydration of intervertebral disks and osteophyte formation can lead to compression of the spinal cord. Degenerative cervical myelopathy (DCM) may result in significantly impaired motor movement and pain, potentially triggering a downward spiral of physical infirmity and social isolation [1, 2]. Studies have shown that spine surgery is the most effective therapy for moderate and severe DCM [3], but the recovery can be limited by irreversible spinal cord damage. Long-term changes within the brain structure may occur to compensate for functional deficits, as has been demonstrated in studies of DCM [4] and traumatic spinal cord injury [5–7].

Current data suggests that spinal cord compression and injury are likely to contribute to the clinical presentation in DCM patients. This has been demonstrated using standard MRI, and more recently confirmed utilizing advanced imaging techniques that have elucidated pathological microstructural [8–10], biochemical [11–13], and ischemic or perfusion [14] spinal cord derangements. Further study has demonstrated that spinal cord injury induces supraspinal alterations in the central nervous system (CNS) including changes in cortical morphometry [14] and brain functional connectivity [15, 16], which have been shown to strongly correlate with neck disability, functional impairment, and surgical outcomes in DCM patients. However, it remains unknown whether the axons connecting these regions within the brain are similarly altered as a result of DCM or whether changes in the brain are merely relate to cortical volition or temporal coherence of functional signaling.

While diffusion tensor imaging (DTI) has been useful for evaluating microscopic structural organization of white matter fibers within the CNS [17–19], it cannot reliably differentiate multiple fiber orientations within the same image voxel [20–22], nor is it sensitive to the complex architecture of cortical white matter. Diffusion spectral imaging (DSI) [23] is an advanced MR technique that uses multiple diffusion sensitizing directions and multiple *b*-values or “shells” to gain sensitivity to axon orientation as well as density [24], even in the presence of crossing axon fibers [25]. We hypothesized that white matter changes are an adaptation to the chronically enhanced spinal afferent input to the brain, helping to maintain a residual sensory and motor function by limiting its deterioration and contributing to its restoration if the disease progression is halted. DSI-based tractography and connectivity analyses may be useful for quantifying cerebral reorganization in DCM and asymptomatic

spinal cord compression patients, thus potentially providing a clinically relevant imaging biomarker for earlier detection and therapeutic intervention.

2. Materials and methods

2.1. Patients

Forty-seven patients with advanced cervical spondylosis (CS) and spinal cord compression were prospectively enrolled from 2016 to 2018 in a cross-sectional study involving observational MRI and evaluation of neck disability. Patients with a history of stroke or cerebral vascular disease were not included in this study. A fellowship trained board certified neuroradiologist with more than 20 years of experience reviewed all brain MRI exams and patients with incidental evidence of cerebrovascular disease were further excluded from subsequent analyses. Of the 47 patients, 38 had DCM and 9 were neurologically asymptomatic (mJOA =18). The patient cohort ranged from 37 to 81 years old, with an average age of 58. All patients were recruited from an outpatient neurosurgery clinic, and had spinal cord compression with evidence of spinal cord deformation and an absence of visible cerebrospinal fluid signal around the spinal cord at the site of maximal compression on MRI. The patients were referred for neurosurgical evaluation of the documented cervical stenosis, and presented either neurological symptomatology, neck pain, or both. All patients signed Institutional Review Board-approved consent forms, and all analyses were performed in compliance with the Health Insurance Portability and Accountability Act (HIPAA). A control group of 28 neurologically intact, healthy controls (HCs) volunteered to undergo the same MRI protocol. The HC cohort ranged from 23 to 64 years old, with an average age of 36. Patient and control demographic data are summarized in Table 1.

The modified Japanese Orthopedic Association (mJOA) scale was used as a measure of neurological function [28], in which a lower mJOA value represents a poorer neurological state. The neck disability index (NDI) score was used as a measure of neck pain and disability [26, 27], in which a higher NDI value represents a more severe neck disability.

2.1.1. Presenting symptoms—The most common presenting symptom was paresthesias or pain in the upper extremities, and was encountered in 38 patients. 36 patients endorsed a history of neck pain. Gait dysfnction was encountered in 20 patients. 19 patients presented with deterioration of hand function. This was most commonly manifested by significant changes in their ability to perform certain activities of daily living such as using utensils, writing, sewing, and buttoning buttons. 2 patients presented with recent changes in bladder function.

2.1.2. Physical examination—16 patients were noted to have weakness in the upper extremities on examination, and 2 had weakness in the lower extremities. 14 patients had decreased sensation in the upper extremities, and 2 had sensory changes in the lower extremities. Hyperreflexia was the most common upper motor neuron sign, and was found in 22 patients. Hoffman’s sign was the second most common, and was observed in 21 patients. 8 patients had clonus in the lower extremities, and 5 had a positive Babinski reflex.

2.1.3. Radiographical imaging—Standard cervical spine MRI was obtained in the entire patient cohort, and revealed spinal cord compression and absence of visible cerebrospinal fluid at the level of maximum compression in each case (Fig. 1). The spinal canal narrowing was related to advanced cervical spondylosis manifested by a combination of facet arthropathy, ligamentum flavum hypertrophy, and varying degrees of ventral discosteophyte compression. 27 of the patients had a lordotic cervical spine, 13 had straight, and 7 had a kyphotic spinal alignment. 32 patients had T2-weighted signal abnormalities located within the spinal cord parenchyma and 15 were without signal changes.

2.2. Diffusion spectral imaging (DSI) acquisition

All DSI data was collected on a Siemens Prisma 3T MR scanner (Siemens Healthcare, Erlangen, Germany) with a repetition time of (TR)=6.9–12.5sec, an echo time of (TE)=93msec, a flip angle of 90^{o}, and a field-of-view (FOV) of 245 × 245mm with an acquisition matrix of 160 × 160 for a voxel size of 1.5mm x 1.5mm x 2.5mm. A total of 61 samples were acquired with diffusion sensitizing gradients applied in two different acquisition schemes as summarized in Table 2. 19 patients underwent the first acquisition scheme with maximum b-value of 3000 s/mm^2, while 28 patients underwent the second acquisition scheme with maximum b-value of 2000 s/mm^2.

2.3. Image post-processing and statistical analysis

Following acquisition, all diffusion-weighted images were de-noised using *MRtrix3* package (http://www.mrtrix.org) [29]. The FMRIB Software Library's Diffusion Toolbox (FDT) (www.fmrib.ox.ac.uk/fsl) was then used to correct for eddy current and patient movement during image acquisition. Quantitative anisotropy (QA) from the spin distribution function (SDF) was calculated using the *q*-space diffeomorphic reconstruction (QSDR) [30, 31], a modeless reconstruction approach that applies spatial normalization to diffusion data, with a diffusion sampling length ratio of 1.25. Local connectomes were then mapped using generalized fractional anisotropy (GFA) and normalized quantitative anisotropy (NQA) values at the voxel level as described below.

Diffusion MRI connectometry [32, 33] was used to evaluate potential associations between imaging parameters and symptoms presented by DCM and asymptomatic spinal cord compression patients, including neck disability and impaired neurological function. Age was included as a covariate in the statistical analysis of the microstructural changes to account for the effect of age on structural connectivity and integrity, as well as the difference in age between the patient and HC groups. The GFA image and the NQA image for each participant were registered to the Johns Hopkins University DTI atlas (ICBM-DTI-81 1mm FA atlas) using FSL. A multiple linear regression model was created using AFNI's *3dttest++* function, with covariates including NDI, mJOA, and age data for both patients and HCs. For each T-test, permutation test was performed to by estimating data smoothness through command *3dFWHMx* in AFNI, and then the cluster threshold was evaluated at a level of significance, $p<0.05$ through command *3dClustSim* in AFNI. The image processing and statistical analysis pipeline is shown graphically in Fig. 2.

3. Results

3.1. Comparison between patients and HCs

The mean mJOA score of the entire patient cohort was 15.8, with a range from 9–18. The mean NDI score was 10.8, with a range from 0–37. Within the patient cohort, the mean mJOA score for the DCM patients was 14.6, and mean NDI was 12. The mean mJOA score for the neurologically asymptomatic patients with spinal cord compression was 18, with an NDI of 7.

Regional differences in DSI between patients and HCs were compared by obtaining the spin distribution function and correcting for age and symptom scores. Generally, GFA measurements tended to be higher in HCs than in the patient cohort (Fig. 3A). Higher GFA was observed in structures responsible for sensory and motor integration, including the cerebellar and cerebral peduncles, the genu and splenium of the corpus callosum, and certain fiber tracts. Specifically, complex white matter fibers in the frontal lobe, corticospinal and spinothalamic tracts, and the anterior, posterior and superior regions of the corona radiata fibers exhibit increased GFA. When examining NQA, most regions were significantly higher in patients than in the HCs (Fig. 3B). Particularly, the body and the splenium of the corpus callosum, together with corona radiata, exhibited large areas of higher NQA in the patient cohort than in the HCs. In contrast, the right genu of the corpus callosum showed a lower NQA in patients than in the HCs. Interestingly, both enhanced and reduced NQA values were observed in patients along certain complex tracts including posterior thalamic radiation fibers and sagittal stratum fibers when compared to HCs. These results support the hypothesis that patients exhibit widespread white matter changes within the cerebral brain.

3.2. Correlation between DSI and symptom severity in patients

To test the hypothesis that cerebral reorganization within white matter tracts may reflect symptom severity in patients, we explored the correlation between NQA measurements and two major clinical scores (mJOA and NDI) by controlling for the subjects' ages and acquisition schemes. The correlation matrix associating NQA values with symptom scores revealed a distinctive stratification pattern of symptoms as they corresponded to specific anatomical regions (Fig. 4 and Fig. 5). In general, a lower mJOA score tended to correlate with higher NQA values within regions related to sensory and motor systems. For the correlation of the patient cohort, the left superior longitudinal fasciculus fibers, the splenium of corpus callosum, and most of complex tracts including external capsule fibers, anterior, posterior and superior corona radiata fibers were associated with worsened neurological status as measured by mJOA, as illustrated in Fig. 4A and summarized in Table 3. By including the HC cohort, left retro-lenticular part of internal capsule was also associated with decreasing mJOA, as illustrated in Fig. 4B and summarized in Table 3.

Additionally, connectometry analysis of the patient cohort identified both positive and negative associations between NDI scores and NQA measures. As shown in Fig. 5A and summarized in Table 4, complex fibers including the posterior corona radiata and the posterior limb of internal capsule showed a positive correlation between NDI scores and NQA, while most supratentorial regions connected by the splenium of the corpus callosum,

the superior corona radiata, and the associative fibers showed a negative correlation between NDI scores and NQA. By including the HC cohort, we observed a positive correlation between NDI scores and NQA in both infratentorial and supratentorial brain. Specifically, the splenium of the corpus callosum, the posterior limb of internal capsule, and other complex fibers showed increased NQA values with large cluster volumes.

To further demonstrate the association between structural connectivity and two major clinical measures of function and disability (mJOA and NDI, respectively), connectometry analysis was performed on the patient cohort using only the second acquisition protocol with a maximum b-value of 2000 s/mm^2 (Note inclusion of patients with both acquisition schemes will result in significant differences in connectivity based solely on the particular acquisition scheme). Consistent with the results in Fig. 3A, GFA values calculated from anatomical regions, including posterior and superior corona radiata fibers, were found to correlate with increasing mJOA and NDI scores. GFA values calculated from anatomical regions, including the body and genu of the corpus callosum and the anterior and superior regions of the corona radiata, were found to correlate with decreasing mJOA scores. Most complex fibers and corticospinal tracts were found to correlate with decreasing NDI scores (Fig. 6, Table 5). For analysis of the patient and HC cohorts who underwent the first acquisition protocol with a maximum b-value of 3000 s/mm^2, NQA values showed a negative association with mJOA and a positive association with NDI in regions previously identified (Fig. 7, Table 6), which are consistent with results presented in Fig. 4B and Fig. 5B. To demonstrate the extent of microstructural alterations associated with symptom scores, scatter plots of representative correlation between measured mJOA/NDI and DSI from specific cerebral white matter regions are illustrated on the right column of Fig. 6 and Fig. 7. GFA values calculated from both the left cingulum fibers and the right posterior corona radiata fibers showed positive linear correlation with mJOA with R^2 values of 0.3189 and 0.2882, while GFA values calculated from both the right corticospinal tract and the right posterior corona radiata fibers showed negative linear correlation with NDI with R^2 values of 0.2457 and 0.1940. In contrast, NQA values calculated from both the right cingulum fibers and the right posterior corona radiata fibers showed negative linear correlation with mJOA with R^2 values of 0.2359and 0.2935. NQA values calculated from both right posterior thalamic radiation fibers and the right posterior corona radiata fibers showed positive linear correlation with NDI with R^2 values of 0.2094 and 0.1889.

Additional analysis was performed within the patient cohort to identify association between T2 hyperintensity signal change in spine cord and cortical changes (Fig. S1). Patients without spinal cord signal change had overall higher GFA values throughout most of the brain compared to patients with spinal cord signal changes. Additionally, the infratentorial regions of the brain, the brainstem and the basal ganglia showed a higher value of NQA in patients without signal changes in spine cord, while the supratentorial regions, especially the prefrontal, frontal, parietal lobes, as well as superior part of the brain showed a higher value of NQA in patients with signal changes in the spinal cord.

4. Discussion

As chronic spinal compression can result in irreversible damage, including both neuronal and white matter demyelination [1], the majority of DCM research has focused on changes within the spinal cord itself at the site of compression [34]. DTI has been particularly helpful in providing a quantitative assessment of spinal cord injury in DCM patients [7–9]. Only recently have DCM investigations begun to note changes within the brain including alterations in cortical morphometry [14], microstructure [35, 36], and brain functional connectivity [15] associated with neck disability and functional impairment. In particular, these studies have noted a decrease in cortical thickness and an increase in functional connectivity between primary sensorimotor and supplemental motor or sensory regions. Consistent with these observations, we observed significant alterations in white matter tracts connecting primary motor and sensory cortices following correction for clinical and age differences.

4.1. Differences in white matter alterations between patients and HCs

Studies have demonstrated cerebral alterations in patients with spinal cord injury through DTI [37–39]. However, DTI cannot directly image multiple fiber orientations within a single voxel. By applying multiple magnetic gradients along various directions, DSI enables us to visualize the complex fiber architecture. GFA as measured by DSI is highly correlated with FA and is indicative of demyelination, axonal loss, edema, or inflammation. After adjusting for age differences and symptom severity, results showed overall reduced GFA in the patient cohort compared to HCs, indicating that these patients have lowered directional coherence from axonal or dendritic projections throughout the brain. These alterations were observed in specific regions of the brain involved in sensory processing, including white matter tracts connecting the cingulate, temporal lobes, somatosensory integration areas, and frontal/prefrontal cortical projections. These findings are consistent with reported brain atrophy and white matter damage in patients with DCM [38, 40], especially in primary sensorimotor areas and SMA.

Our results support the hypothesis that cervical spinal cord compression or injury may damage the white matter integrity of DCM patients, causing atrophy of the sensorimotor cortex and thalami. Significant microstructural alterations occurring within the basal ganglia, thalamus, frontal and parietal lobes indicate an imbalance of the cortico-basal ganglia-thalamus-cortical loop in motor regulation and pain modulation, which is also observed in other chronic pain syndromes. In addition, reduced GFA values in DCM and asymptomatic spinal cord compression patients along the corticospinal tracts, including regions extending through the corona radiata and internal capsule, complement previous studies in which demyelination of the ascending and descending corticospinal fibers appear to be the predominant pathological mechanism in this patient population [41]. The progressive loss of axonal conduction along these pathways seems to play an important role in the pathogenesis of DCM, as fiber integrity is associated with the clinical symptoms.

Although the DCM and asymptomatic spinal cord compression patients showed overall lower GFA compared to HCs, we observed increased NQA in specific areas including the internal capsule, corona radiata, and posterior thalamic radiation. The internal capsule/

corona radiata pathway contains ascending fibers from the thalamus up to the cortex and descending fibers from the frontal and parietal lobes down to subcortical regions, serving as the anatomic linkage to support cognitive, perceptual, and motor systems in the cortex. Consistent with several recent observations of cerebral reorganization, NQA quantified higher connectivity within regions associated with somatosensory function, indicating possible structurally adaptive changes as a compensatory mechanism for neurological dysfunction caused by white matter degeneracy of DCM patients. DTI-based tractography of SCI animals revealed the presence of new fibers in the internal capsule and cerebral peduncles [39], which are involved in the planning and initiating of movement, coordinating fine motor movements, and conveying sensory information. Similarly, fMRI studies in DCM patients showed increased functional connectivity within sensorimotor regions with increasing neurological impairment, including the precentral gyrus, postcentral gyrus, and supplemental motor regions [15].

4.2. Correlation of white matter changes with symptoms

We have shown that the complex relationship between structural reorganization and disease progression within DCM patients extends far beyond the spinal cord. Correlating DSI measures with clinical conditions will enable us to better understand the nature of specific cerebral changes that occur in the pathogenesis of CS.

4.2.1. Neurological Status—Consistent with results observed in the significant connectivity adaptions and microstructural alterations between the patient cohort and the HCs, we found a lower mJOA score tended to correlate with a higher NQA and a lower GFA in the corpus callosum and in common complex tracts such as corona radiata. Surprisingly, the internal capsule, posterior thalamic radiation, and superior longitudinal fasciculus pathways demonstrated increased fiber density with worsened neurological status before the microstructural alterations had started to take place, since the association between the fiber integrity (measured by GFA) and the neurological status was not observed in those regions. The presence of new fibers presumably provided connectivity between different anatomical structures, explaining the greater functional activation observed on fMRI in DCM patients [42–45].

4.2.2. Neck disability—Although a negative correlation between NDI and NQA was observed in the patient cohort along the sagittal striatum tracts and associated fibers responsible for relaying and integrating information, we also observed that NDI was negatively correlated with GFA and positively correlated with NQA along the corticospinal tract passing the basal ganglia, thalamus and extending through the corona radiata. This motor dysfunction as well as motor cortex stimulation has been reported over a wide variety of chronic pain conditions [46–48]. We have previously demonstrated that the motor cortex of CS patients can be involved in both neurological symptoms and chronic pain [15, 16], where a strong activity was associated with worsening neck disability within precentral gyri and the SMA. Our findings suggest that the white matter integrity of DCM patients may be damaged and that with insufficient sensory and motor input, structural connectivity to the thalamus and somatosensory cortex is enhanced to compensate for neurological dysfunction. Such cerebral reorganization is supported by previous findings of increased functional

connectivity between thalami and the sensorimotor cortex during myelopathy [49]. as well as increased cortical activity within premotor, primary somatosensory, and parietal-integrated areas [50] in response to loss of somatosensory input.

4.3. Limitations

Results from the current study have meaningful clinical implications, suggesting that spinal cord damage can lead to measurable microstructural changes within cerebral areas responsible for motor activity regulation and sensory information processing. Longitudinal studies are still required to determine whether the plasticity of the cerebral changes in patients who become symptomatic arise spontaneously or in response to specific therapies. Additionally, this study is an exploratory analysis, and a larger sample size is necessary to verify if these changes can reflect and measure overall disease severity in DCM patients, as well as differentiate those with asymptomatic spinal cord compression. Finally, although age was included as a covariate in the statistical analysis of microstructural differences between patient and HC groups, there were marked differences between these groups. While age-matched data including data from older HC's or additional younger DCM patients would be useful in making a comparison between two groups that are closer in age, DCM is an age-related disorder and degenerative changes from spinal cord compression are likely intertwined.

5. Conclusions

Spinal cord compression can induce microstructural alterations in cerebral white matter tracts. Our results suggest that the GFA and NQA values in DSI are closely related to the severity of neurological impairment. Future study will determine whether these advanced imaging methods may enable clinicians to more accurately predict potential surgical and therapeutic outcomes for patients with DCM.

Supplementary Material

Refer to Web version on PubMed Central for supplementary material.

Grant Funding:

Funding was received through the following NIH/NINDS grants: 1R01NS078494-01A1 (to LTH, NS, and BME), and 2R01NS078494-06 (to LTH, NS, and BME)

References

[1]. Kalsi-Ryan S, Karadimas SK, Fehlings MG. Cervical spondylotic myelopathy: the clinical phenomenon and the current pathobiology of an increasingly prevalent and devastating disorder. Neuroscientist 2013;19:409–21. [PubMed: 23204243]

[2]. Tracy JA, Bartleson JD. Cervical spondylotic myelopathy. Neurologist 2010;16:176–87. [PubMed: 20445427]

[3]. Fehlings MG, Tetreault LA, Riew KD, Middleton JW, Aarabi B, Arnold PM, et al. A Clinical Practice Guideline for the Management of Patients With Degenerative Cervical Myelopathy: Recommendations for Patients With Mild, Moderate, and Severe Disease and Nonmyelopathic Patients With Evidence of Cord Compression. Global Spine J 2017;7:70S–83S. [PubMed: 29164035]

[4]. Zdunczyk A, Schwarzer V, Mikhailov M, Bagley B, Rosenstock T, Picht T, et al. The Corticospinal Reserve Capacity: Reorganization of Motor Area and Excitability As a Novel Pathophysiological Concept in Cervical Myelopathy. Neurosurgery 2018;83:810–8. [PubMed: 29165642]

[5]. Curt A, Bruehlmeier M, Leenders KL, Roelcke U, Dietz V. Differential effect of spinal cord injury and functional impairment on human brain activation. J Neurotrauma 2002;19:43–51. [PubMed: 11852977]

[6]. Yoon EJ, Kim YK, Shin HI, Lee Y, Kim SE. Cortical and white matter alterations in patients with neuropathic pain after spinal cord injury. Brain Res 2013;1540:64–73. [PubMed: 24125807]

[7]. Nardone R, Holler Y, Brigo F, Seidl M, Christova M, Bergmann J, et al. Functional brain reorganization after spinal cord injury: systematic review of animal and human studies. Brain Res 2013;1504:58–73. [PubMed: 23396112]

[8]. Ellingson BM, Salamon N, Grinstead JW, Holly LT. Diffusion tensor imaging predicts functional impairment in mild-to-moderate cervical spondylotic myelopathy. Spine J 2014;14:2589–97. [PubMed: 24561036]

[9]. Ellingson BM, Salamon N, Woodworth DC, Holly LT. Correlation between degree of subvoxel spinal cord compression measured with super-resolution tract density imaging and neurological impairment in cervical spondylotic myelopathy. J Neurosurg Spine 2015;22:631–8. [PubMed: 25746116]

[10]. Ellingson BM, Salamon N, Woodworth DC, Yokota H, Holly LT. Reproducibility, temporal stability, and functional correlation of diffusion MR measurements within the spinal cord in patients with asymptomatic cervical stenosis or cervical myelopathy. J Neurosurg Spine 2018;28:472–80. [PubMed: 29424671]

[11]. Salamon N, Ellingson BM, Nagarajan R, Gebara N, Thomas A, Holly LT. Proton magnetic resonance spectroscopy of human cervical spondylosis at 3T. Spinal Cord 2013;51:558–63. [PubMed: 23588574]

[12]. Ellingson BM, Salamon N, Hardy AJ, Holly LT. Prediction of Neurological Impairment in Cervical Spondylotic Myelopathy using a Combination of Diffusion MRI and Proton MR Spectroscopy. PLoS One 2015;10:e0139451. [PubMed: 26431174]

[13]. Holly LT, Ellingson BM, Salamon N. Metabolic Imaging Using Proton Magnetic Spectroscopy as a Predictor of Outcome After Surgery for Cervical Spondylotic Myelopathy. Clin Spine Surg 2017;30:E615–E9. [PubMed: 28525487]

[14]. Woodworth DC, Holly LT, Mayer EA, Salamon N, Ellingson BM. Alterations in Cortical Thickness and Subcortical Volume are Associated With Neurological Symptoms and Neck Pain in Patients With Cervical Spondylosis. Neurosurgery 2019;84:588–98. [PubMed: 29548020]

[15]. Woodworth DC, Holly LT, Salamon N, Ellingson BM. Resting-State Functional Magnetic Resonance Imaging Connectivity of the Brain Is Associated with Altered Sensorimotor Function in Patients with Cervical Spondylosis. World Neurosurg 2018;119:e740–e9. [PubMed: 30092474]

[16]. Holly LT, Wang C, Woodworth DC, Salamon N, Ellingson BM. Neck disability in patients with cervical spondylosis is associated with altered brain functional connectivity. J Clin Neurosci 2019;69:149–54. [PubMed: 31420276]

[17]. Basser PJ, Mattiello J, LeBihan D. MR diffusion tensor spectroscopy and imaging. Biophys J 1994;66:259–67. [PubMed: 8130344]

[18]. Mori S, Crain BJ, Chacko VP, van Zijl PC. Three-dimensional tracking of axonal projections in the brain by magnetic resonance imaging. Ann Neurol 1999;45:265–9. [PubMed: 9989633]

[19]. Conturo TE, Lori NF, Cull TS, Akbudak E, Snyder AZ, Shimony JS, et al. Tracking neuronal fiber pathways in the living human brain. Proc Natl Acad Sci U S A 1999;96:10422–7. [PubMed: 10468624]

[20]. Basser PJ, Pajevic S, Pierpaoli C, Duda J, Aldroubi A. In vivo fiber tractography using DT-MRI data. Magn Reson Med 2000;44:625–32. [PubMed: 11025519]

[21]. Lazar M, Alexander AL. An error analysis of white matter tractography methods: synthetic diffusion tensor field simulations. Neuroimage 2003;20:1140–53. [PubMed: 14568483]

[22]. Tournier JD, Calamante F, King MD, Gadian DG, Connelly A. Limitations and requirements of diffusion tensor fiber tracking: an assessment using simulations. Magn Reson Med 2002;47:701–8. [PubMed: 11948731]

[23]. Wedeen VJ, Hagmann P, Tseng WY, Reese TG, Weisskoff RM. Mapping complex tissue architecture with diffusion spectrum magnetic resonance imaging. Magn Reson Med 2005;54:1377–86. [PubMed: 16247738]

[24]. Schmahmann JD, Pandya DN, Wang R, Dai G, D'Arceuil HE, de Crespigny AJ, et al. Association fibre pathways of the brain: parallel observations from diffusion spectrum imaging and autoradiography. Brain 2007;130:630–53. [PubMed: 17293361]

[25]. Wedeen VJ, Wang RP, Schmahmann JD, Benner T, Tseng WY, Dai G, et al. Diffusion spectrum magnetic resonance imaging (DSI) tractography of crossing fibers. Neuroimage 2008;41:1267–77. [PubMed: 18495497]

[26]. Vernon H The Neck Disability Index: state-of-the-art, 1991–2008. J Manipulative Physiol Ther 2008;31:491–502. [PubMed: 18803999]

[27]. Vernon H, Mior S. The Neck Disability Index: a study of reliability and validity. J Manipulative Physiol Ther 1991;14:409–15. [PubMed: 1834753]

[28]. Benzel EC, Lancon J, Kesterson L, Hadden T. Cervical laminectomy and dentate ligament section for cervical spondylotic myelopathy. J Spinal Disord 1991;4:286–95. [PubMed: 1802159]

[29]. Calamante F, Tournier JD, Smith RE, Connelly A. A generalised framework for super-resolution track-weighted imaging. Neuroimage 2012;59:2494–503. [PubMed: 21925280]

[30]. Yeh FC, Tseng WY. NTU-90: a high angular resolution brain atlas constructed by q-space diffeomorphic reconstruction. Neuroimage 2011;58:91–9. [PubMed: 21704171]

[31]. Yeh FC, Wedeen VJ, Tseng WY. Estimation of fiber orientation and spin density distribution by diffusion deconvolution. Neuroimage 2011;55:1054–62. [PubMed: 21232611]

[32]. Yeh FC, Badre D, Verstynen T. Connectometry: A statistical approach harnessing the analytical potential of the local connectome. Neuroimage 2016;125:162–71. [PubMed: 26499808]

[33]. Yeh FC, Tang PF, Tseng WY. Diffusion MRI connectometry automatically reveals affected fiber pathways in individuals with chronic stroke. Neuroimage Clin 2013;2:912–21. [PubMed: 24179842]

[34]. Ellingson BM, Salamon N, Holly LT. Advances in MR imaging for cervical spondylotic myelopathy. Eur Spine J 2015;24 Suppl 2:197–208. [PubMed: 23917647]

[35]. Severino R, Nouri A, Tessitore E. Degenerative Cervical Myelopathy: How to Identify the Best Responders to Surgery? J Clin Med 2020;9.

[36]. Martin AR, De Leener B, Cohen-Adad J, Cadotte DW, Nouri A, Wilson JR, et al. Can microstructural MRI detect subclinical tissue injury in subjects with asymptomatic cervical spinal cord compression? A prospective cohort study. BMJ Open 2018;8:e019809.

[37]. Sun P, Murphy RK, Gamble P, George A, Song SK, Ray WZ. Diffusion Assessment of Cortical Changes, Induced by Traumatic Spinal Cord Injury. Brain Sci 2017;7.

[38]. Bernabeu-Sanz A, Molla-Torro JV, Lopez-Celada S, Moreno Lopez P, Fernandez-Jover E. MRI evidence of brain atrophy, white matter damage, and functional adaptive changes in patients with cervical spondylosis and prolonged spinal cord compression. Eur Radiol 2019.

[39]. Ramu J, Herrera J, Grill R, Bockhorst T, Narayana P. Brain fiber tract plasticity in experimental spinal cord injury: diffusion tensor imaging. Exp Neurol 2008;212:100–7. [PubMed: 18482724]

[40]. Kowalczyk I, Duggal N, Bartha R. Proton magnetic resonance spectroscopy of the motor cortex in cervical myelopathy. Brain 2012;135:461–8. [PubMed: 22180462]

[41]. Fehlings MG, Skaf G. A review of the pathophysiology of cervical spondylotic myelopathy with insights for potential novel mechanisms drawn from traumatic spinal cord injury. Spine (Phila Pa 1976) 1998;23:2730–7. [PubMed: 9879098]

[42]. Ramu J, Bockhorst KH, Grill RJ, Mogatadakala KV, Narayana PA. Cortical reorganization in NT3-treated experimental spinal cord injury: Functional magnetic resonance imaging. Exp Neurol 2007;204:58–65. [PubMed: 17112518]

[43]. Ramu J, Bockhorst KH, Mogatadakala KV, Narayana PA. Functional magnetic resonance imaging in rodents: Methodology and application to spinal cord injury. J Neurosci Res 2006;84:1235–44. [PubMed: 16941500]

[44]. Dong Y, Holly LT, Albistegui-Dubois R, Yan X, Marehbian J, Newton JM, et al. Compensatory cerebral adaptations before and evolving changes after surgical decompression in cervical spondylotic myelopathy. J Neurosurg Spine 2008;9:538–51. [PubMed: 19035745]

[45]. Holly LT, Dong Y, Albistegui-DuBois R, Marehbian J, Dobkin B. Cortical reorganization in patients with cervical spondylotic myelopathy. J Neurosurg Spine 2007;6:544–51. [PubMed: 17561743]

[46]. Martucci KT, Ng P, Mackey S. Neuroimaging chronic pain: what have we learned and where are we going? Future Neurol 2014;9:615–26. [PubMed: 28163658]

[47]. Flodin P, Martinsen S, Altawil R, Waldheim E, Lampa J, Kosek E, et al. Intrinsic Brain Connectivity in Chronic Pain: A Resting-State fMRI Study in Patients with Rheumatoid Arthritis. Front Hum Neurosci 2016;10:107. [PubMed: 27014038]

[48]. Antal A, Terney D, Kuhnl S, Paulus W. Anodal transcranial direct current stimulation of the motor cortex ameliorates chronic pain and reduces short intracortical inhibition. J Pain Symptom Manage 2010;39:890–903. [PubMed: 20471549]

[49]. Zhou F, Wu L, Liu X, Gong H, Luk KD, Hu Y. Characterizing Thalamocortical Disturbances in Cervical Spondylotic Myelopathy: Revealed by Functional Connectivity under Two Slow Frequency Bands. PLoS One 2015;10:e0125913. [PubMed: 26053316]

[50]. Zhou F, Gong H, Chen Q, Wang B, Peng Y, Zhuang Y, et al. Intrinsic Functional Plasticity of the Thalamocortical System in Minimally Disabled Patients with Relapsing-Remitting Multiple Sclerosis. Front Hum Neurosci 2016;10:2. [PubMed: 26834600]

Highlights

- Brain DSI in DCM, asymptomatic patients, and healthy volunteers were evaluated.
- NDI and mJOA scores were correlated with microstructural changes in the brain.
- DCM and asymptomatic patients had alterations in specific white matter tracts.
- DCM and asymptomatic patients had enhanced connectivity within sensorimotor areas.

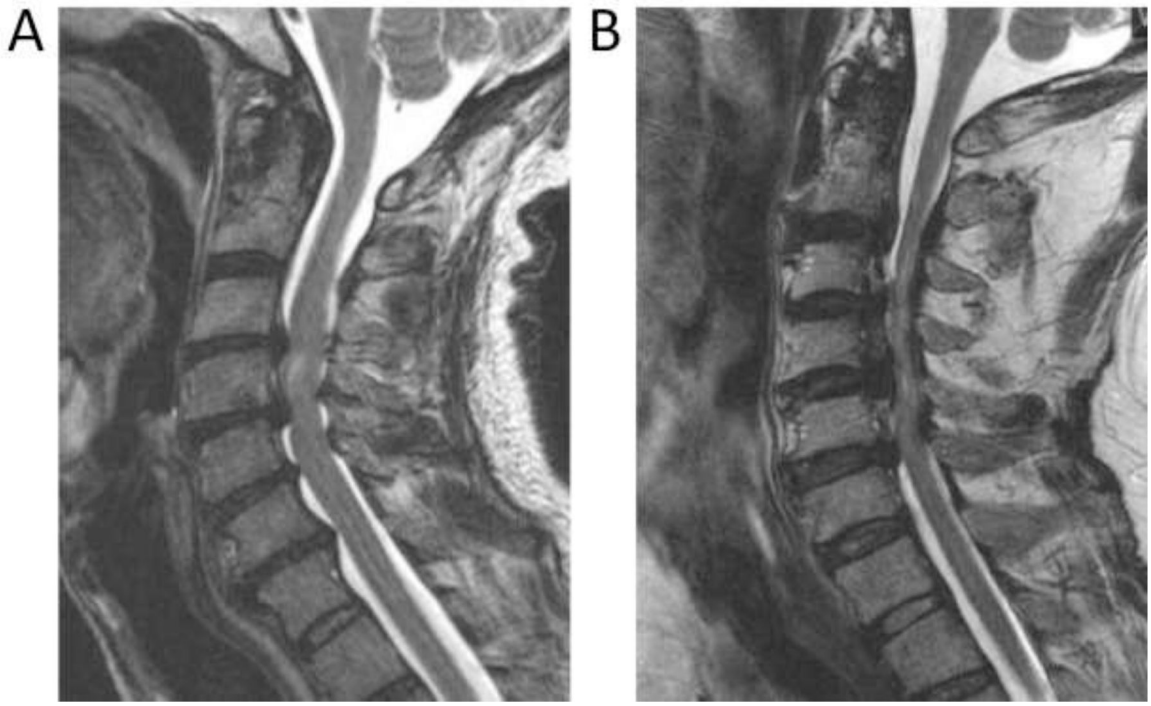

Fig. 1.

A) T2 sagittal MRI of a 59-year-old man with a mJOA score of 17 that primarily presented with paresthesias and numbness in his hands demonstrating spinal cord compression and signal change. B) T2 sagittal MRI of a 52-year-old man with a mJOA score of 11 demonstrating OPLL, severe spinal cord compression and signal change.

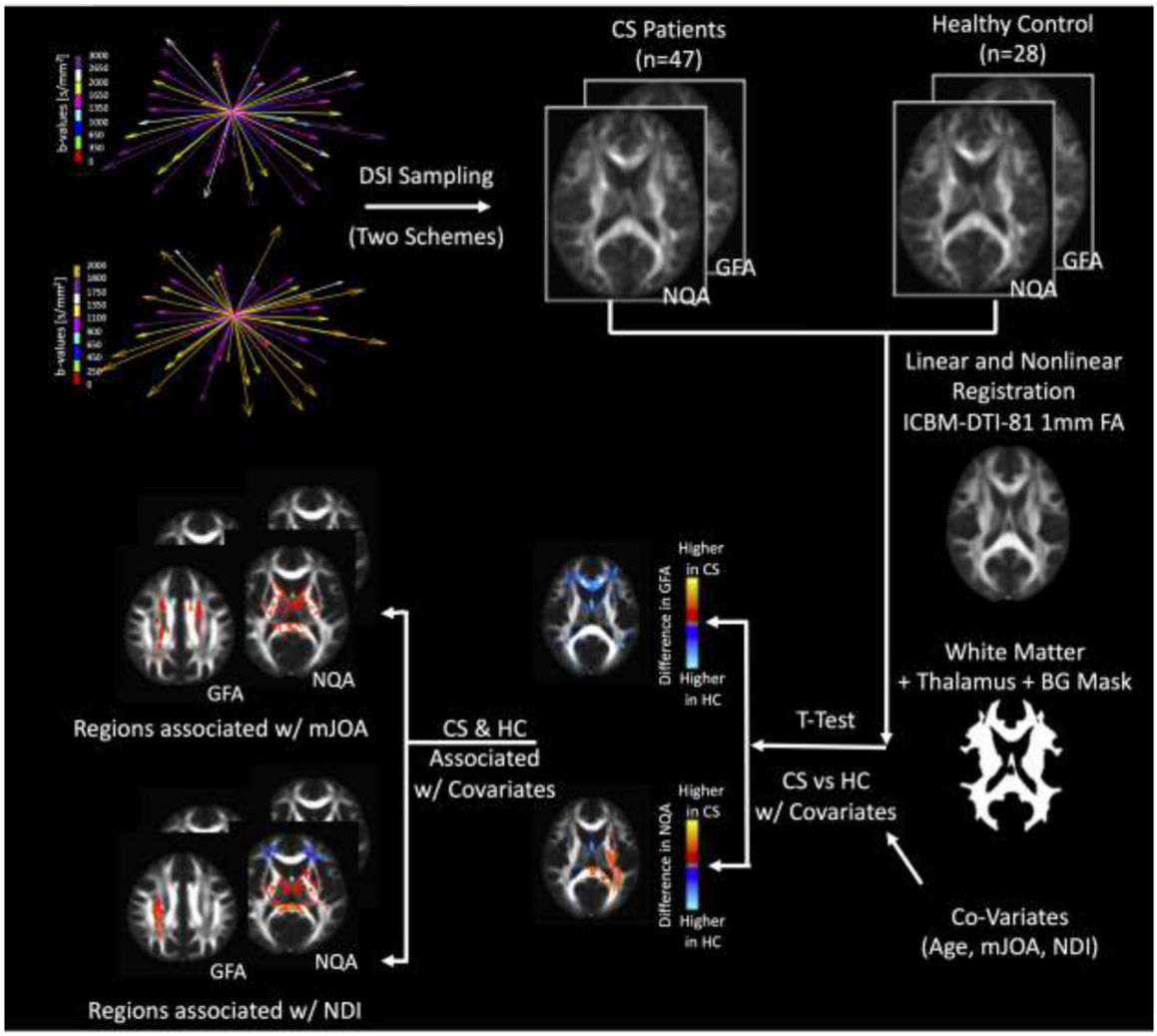

Fig. 2.

Image processing and statistical analysis pipeline for DSI connectometry. Two sampling schemes (maximum b-values 2000 s/mm^2 and 3000 s/mm^2) were used to acquire diffusion weighted images. Both normalized quantitative anisotropy (NQA) and generalized fractional anisotropy (GFA) maps were registered to the ICBM-DTI-81 FA atlas template. T-test with covariates was performed using AFNI (*3dttest++*) in order to compare patients with HCs while considering the acquisition protocol, subjects' ages, NDI and mJOA. Significance was set at $p<0.05$ with a false discovery rate (FDR)<0.05 to identify regions of statistical difference. Additionally, microstructures associated with mJOA and NDI were further investigated within patients and HCs through similar T-test method.

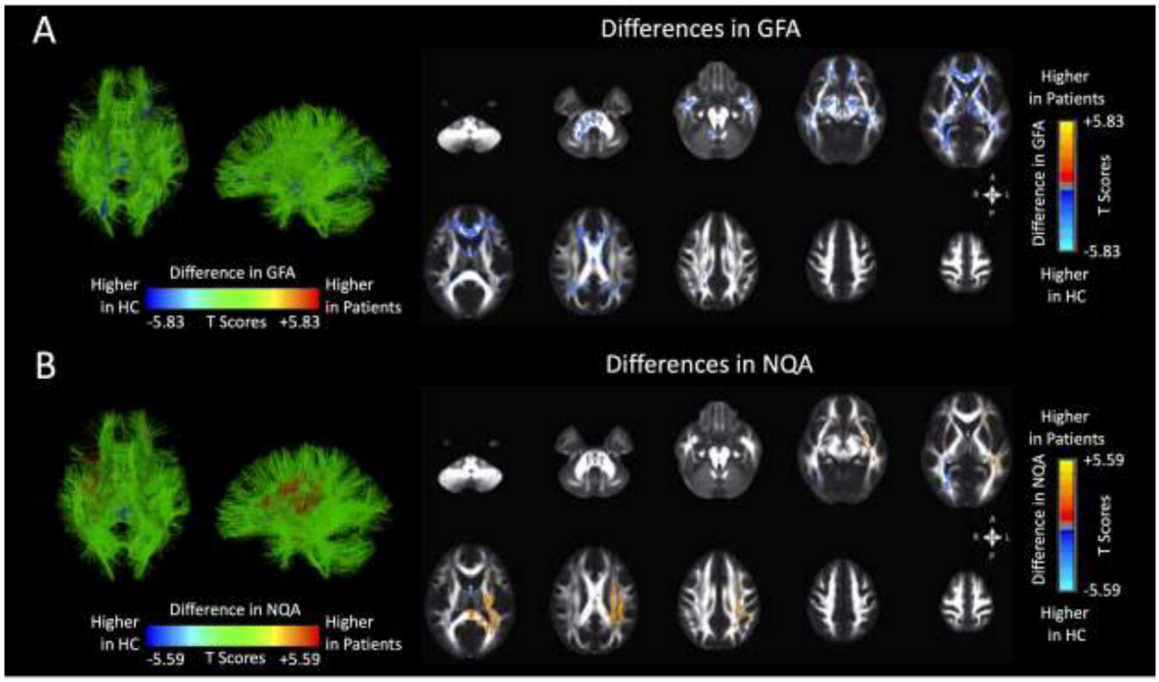

Fig. 3.

Connectometry analysis showing regions of statistical differences in DSI measurements between patients (n=48) and HCs (n=28), with covariates including the acquisition protocol, subjects' ages, NDI and mJOA. A) Observed differences in generalized fractional anisotropy (GFA) values, displayed on axial slices. B) Observed differences in normalized quantitative anisotropy (NQA) values, displayed on axial slices. Significant clusters were determined by thresholding based on level of statistical significance ($p<0.05$) and cluster-based corrections using permutation test. Left column represents differences projected onto cerebral white matter fiber tracts.

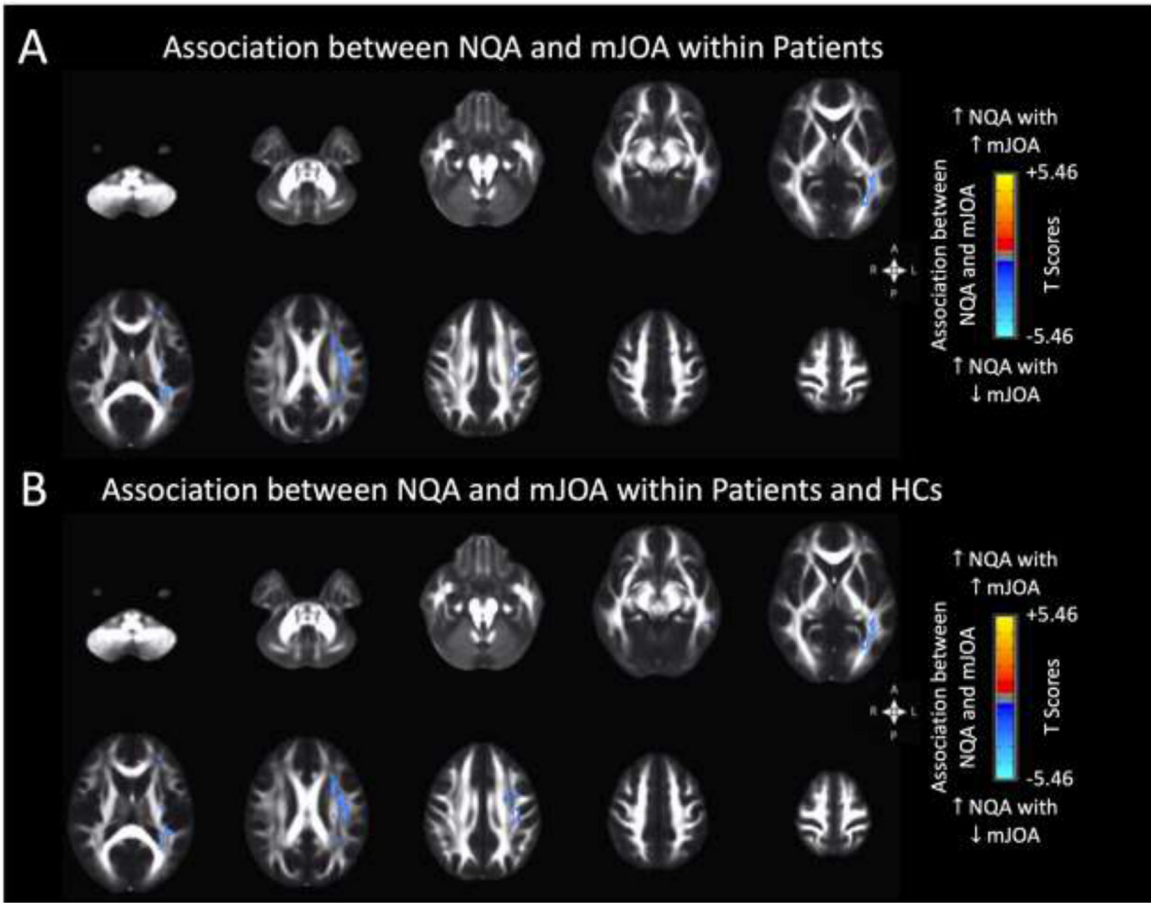

Fig. 4.

Connectometry analysis on NQA by controlling the acquisition protocol, subjects' ages and NDI, showing regions correlated with symptoms of neurological impairment, as measured by the modified Japanese Orthopedic Association (mJOA) score. A) Observed microstructures associated with mJOA scores within patients only, displayed on axial slices. B) Observed microstructures associated with mJOA scores within patients and HCs, displayed on axial slices. Significant clusters were determined by thresholding based on level of statistical significance ($p<0.05$) and cluster-based corrections using permutation test.

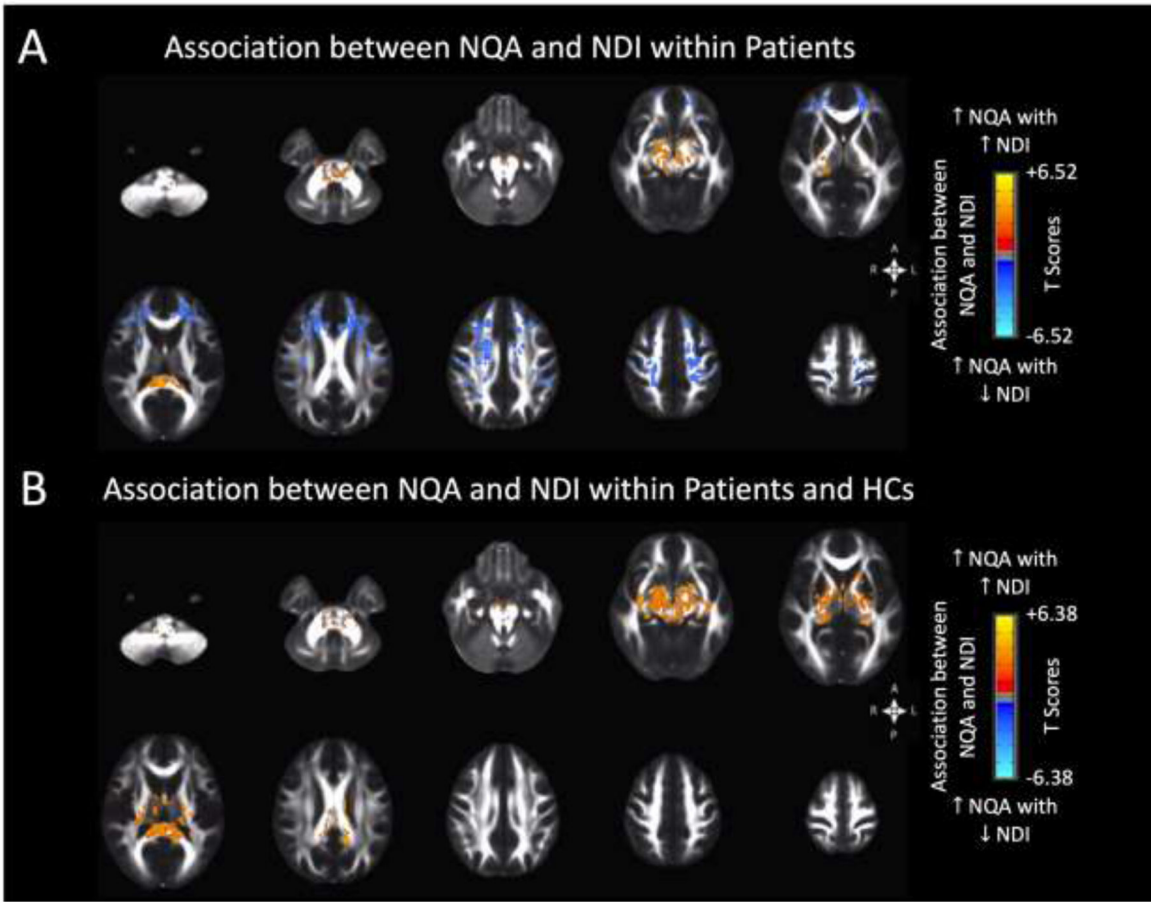

Fig. 5.

Connectometry analysis on NQA by controlling the acquisition protocol, subjects' ages and mJOA, showing regions correlated with the neck pain, as measured by the Neck Disability Index (NDI) score. A) Observed microstructures associated with NDI scores within patients only, displayed on axial slices. B) Observed microstructures associated with NDI scores within patients and HCs, displayed on axial slices. Significant clusters were determined by thresholding based on level of statistical significance ($p<0.05$) and cluster-based corrections using permutation test.

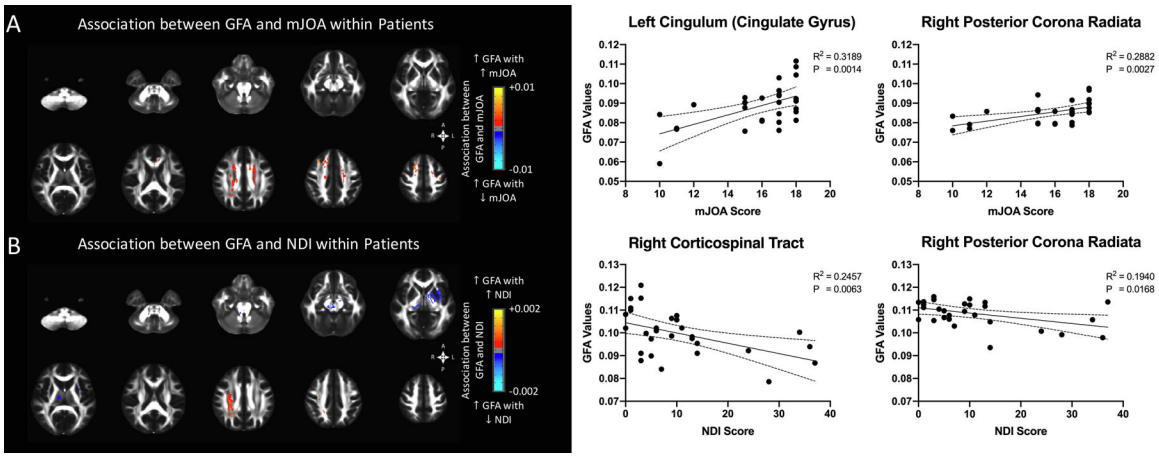

Fig. 6.

Anatomical localization of regions correlated with NDI and mJOA in GFA measurements. Analysis was performed within patients underwent second acquisition protocol with maximum b-value of 2000 s/mm^2. A) Observed microstructures associated with mJOA scores by controlling subjects' ages and NDI, displayed on axial slices. B) Observed microstructures associated with NDI scores by controlling subjects' ages and mJOA, displayed on axial slices. Significant clusters were determined by thresholding based on level of statistical significance ($p<0.05$) and cluster-based corrections using permutation test. Right column illustrates representative correlation between measured mJOA/NDI and cerebral white matters.

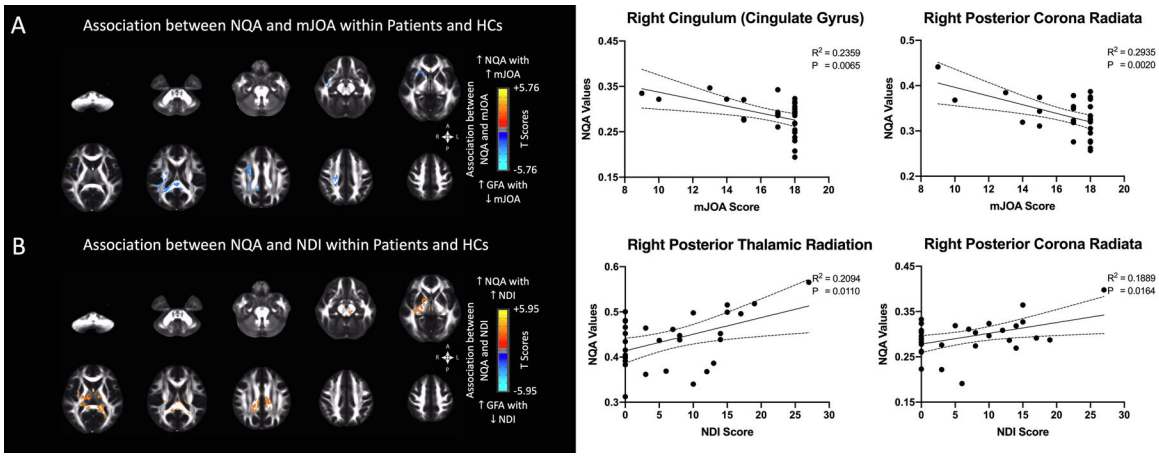

Fig. 7.

Anatomical localization of regions correlated with NDI and mJOA in NQA measurements. Analysis was performed within patients and HCs underwent first acquisition protocol with maximum b-value of 3000 s/mm^2. A) Observed microstructures associated with mJOA scores by controlling subjects' ages and NDI, displayed on axial slices. B) Observed microstructures associated with NDI scores by controlling subjects' ages and mJOA, displayed on axial slices. Significant clusters were determined by thresholding based on level of statistical significance ($p<0.05$) and cluster-based corrections using permutation test. Right column illustrates representative correlation between measured mJOA/NDI and cerebral white matters.

TABLE 1.

Cohort Demographics for Diffusion Spectrum Imaging Analysis.

Subject Population		N	Age (mean years +/− SD) [min, max]	NDI (mean +/− SD) [min, max]	mJOA (mean +/− SD) [min, max]
Patients	asymptomatic spinal cord compression	9	57.2 ± 12.0 [42, 79]	7.0 ± 5.0 [0, 15]	18
	DCM	38	58.4 ± 12.2 [37, 81]	12.0 ± 10.0 [0, 37]	14.6 ± 2.5 [9, 17]
HC Volunteers		28	36.2 ± 14.1 [23, 64]	0	18

DCM = Degenerative Cervical Myelopathy; HC = Healthy control

SD = Standard deviation; mJOA = modified Japanese Orthopedic Association; NDI = Neck Disability Index

TABLE 2.

Diffusion Spectrum Imaging (DSI) Gradient Sampling Scheme.

Acquisition Scheme #1 (N=19)	***b*-Value (s/mm^2)**	0	350	650	1000	1350	1650	2000	2650	3000	-
	Samples/Shell	1	3	6	4	3	12	12	6	15	-
Acquisition Scheme #2 (N=28)	***b*-Value (s/mm^2)**	0	250	450	650	900	1100	1350	1750	1800	2000
	Samples/Shell	1	3	6	4	3	12	12	2	4	15

TABLE 3.

Anatomical regions and corresponding cluster volumes showing significant correlation with the modified Japanese Orthopedic Association (mJOA) score in normalized quantitative anisotropy (NQA) measurement.

Anatomic Regions	Cluster Volume [uL]	
	Patients	Patients and HCs
Lt. Anterior Corona Radiata	178	182
Lt. External Capsule	67	72
Lt. Posterior Corona Radiata	390	361
Lt. Posterior Thalamic Radiation	1147	1049
Lt. Retrolenticular Part of Internal Capsule	287	192
Splenium of Corpus Callosum	301	164
Lt. Superior Corona Radiata	542	974
Lt. Superior Longitudinal Fasciculus	2634	2740

Lt = Left; CS = Cervical spondylosis; HC = Healthy control

TABLE 4.

Anatomical regions and corresponding cluster volumes showing significant correlation with the Neck Disability (NDI) score in normalized quantitative anisotropy (NQA) measurement.

Anatomic Regions	Cluster Volume [uL]	
	Patients	Patients and HCs
Lt. / Rt. Anterior Limb of Internal Capsule	65 / 119	414 / 424
Lt. / Rt. Anterior Corona Radiata	2275 / 1375	-
Body of Corpus Callosum	1107	395
Lt. / Rt. Cerebral Peduncle	468 / 994	1007 / 1516
Lt. / Rt. Cingulum (Cingulate Gyrus)	536 / 133	82 / 69
Lt. / Rt. Corticospinal Tract	24/90	- / 124
Lt. / Rt. External Capsule	54 / 173	310 / 661
Fornix	-	206
Lt. / Rt. Fornix /Stria Terminalis	- / 164	196 / 395
Genu of Corpus Callosum	426	-
Lt. / Rt. Inferior Cerebellar Peduncle	69 / -	94 / 92
Lt. / Rt. Medial Lemniscus	227 / 280	234 / 87
Middle Cerebellar Peduncle	1258	1087
Lt. / Rt. Posterior Limb of Internal Capsule	117 / 564	1566 / 2181
Lt. / Rt. Posterior Corona Radiata	116 / 233	7 / 7
Lt. Posterior Thalamic Radiation	-	14
Lt. / Rt. Retrolenticular Part of Internal Capsule	- / 64	192/ 612
Lt. / Rt. Sagittal Stratum	-	210 / 54
Splenium of Corpus Callosum	2447	4333
Lt. / Rt. Superior Cerebellar Peduncle	-	60 / 30
Lt. / Rt. Superior Corona Radiata	1046/ 1695	5 / 30
Lt. / Rt. Superior Fronto-occipital Fasciculus	67 /60	- / 5
Lt. / Rt. Superior Longitudinal Fasciculus	296 / 356	-
Lt. / Rt. Tapetum	-	55 /9

Lt = Left; Rt = Right; CS = Cervical spondylosis; HC = Healthy control

TABLE 5.

Anatomical regions and corresponding cluster volumes showing significant correlation with the modified Japanese Orthopedic Association (mJOA) score and the Neck Disability (NDI) score in generalized fractional anisotropy (GFA) measurement within patients underwent the second sampling scheme (maximum b-value=2000 s/mm^2).

Anatomic Regions	Cluster Volume [uL]	
	Correlated with mJOA	Correlated with NDI
Lt. Anterior Limb of Internal Capsule	-	132
Lt. / Rt. Anterior Corona Radiata	47 / 67	-
Body of Corpus Callosum	1315	-
Lt. / Rt. Cerebral Peduncle	-	241 / 131
Lt. Cingulum (Cingulate Gyrus)	249	-
Rt. Corticospinal Tract	-	17
Lt. External Capsule	-	927
Genu of Corpus Callosum	485	-
Lt. Inferior Cerebellar Peduncle	-	35
Rt. Medial Lemniscus	-	53
Middle Cerebellar Peduncle	-	14
Lt. / Rt. Posterior Limb of Internal Capsule	-	289 / 31
Lt. / Rt. Posterior Corona Radiata	99 / 439	- / 418
Rt. Superior Cerebellar Peduncle	-	195
Lt. / Rt. Superior Corona Radiata	1099 / 919	- / 448
Rt. Superior Longitudinal Fasciculus	-	358

Lt = Left; Rt = Right; CS = Cervical spondylosis; HC = Healthy control

mJOA = modified Japanese Orthopedic Association; NDI = Neck Disability Index

TABLE 6.

Anatomical regions and corresponding cluster volumes showing significant correlation with the modified Japanese Orthopedic Association (mJOA) score and the Neck Disability (NDI) score in normalized quantitative anisotropy (NQA) measurement within patients and HCs underwent the first sampling scheme (maximum b-value=3000 s/mm^2).

Anatomic Regions	Cluster Volume [uL]	
	Correlated with mJOA	Correlated with NDI
Rt. Anterior Limb of Internal Capsule	123	44
Rt. Anterior Corona Radiata	81	-
Body of Corpus Callosum	333	1504
Lt. / Rt. Cerebral Peduncle	-	68 / 339
Lt. / Rt. Cingulum (Cingulate Gyrus)	- / 76	405 / 831
Rt. Cingulum (Hippocampus)	6	-
Rt. External Capsule	927	537
Fornix	-	132
Lt. / Rt. Fornix /Stria Terminalis	-	29 / 114
Lt. / Rt. Posterior Limb of Internal Capsule	- / 117	46 / 1203
Lt. / Rt. Posterior Corona Radiata	- / 1245	223/ 126
Lt. / Rt. Posterior Thalamic Radiation	- / 94	130 / 29
Lt. / Rt. Retrolenticular Part of Internal Capsule	- / 35	3 / 411
Rt. Sagittal Stratum	74	109
Splenium of Corpus Callosum	1443	3402
Lt. / Rt. Superior Corona Radiata	- / 1689	63 / 3
Rt. Superior Longitudinal Fasciculus	557	-
Rt. Tapetum	82	-

Lt = Left; Rt = Right; CS = Cervical spondylosis; HC = Healthy control

mJOA = modified Japanese Orthopedic Association; NDI = Neck Disability Index